Transfinite mean value interpolation

Christopher Dyken and Michael S. Floater

July 2007, revised November 2007

Abstract

Transfinite mean value interpolation has recently emerged as a simple and robust way to interpolate a function f defined on the boundary of a planar domain. In this paper we study basic properties of the interpolant, including sufficient conditions on the boundary of the domain to guarantee interpolation when f is continuous. Then, by deriving the normal derivative of the interpolant and of a mean value weight function, we construct a transfinite Hermite interpolant and discuss various applications.

Keywords: Transfinite interpolation, Hermite interpolation, mean value coordinates,

1 Introduction

Transfinite interpolation means the construction of a function over a planar domain that matches a given function on the boundary, and has various applications, notably in geometric modelling and finite element methods [20]. Transfinite mean value interpolation has developed in a series of papers [3, 10, 6, 12]. In [3] barycentric coordinates over triangles were generalized to star-shaped polygons, based on the mean value property of harmonic functions. The motivation for these 'mean value coordinates' was to parameterize triangular meshes but they also give a method for interpolating piecewise linear data defined on the boundary of a convex polygon. In [10] it was shown that these mean value interpolants extend to any simple polygon and even sets of polygons, possibly nested, with application to image warping. In both [6] and [12] 3D coordinates were similarly constructed for closed triangular meshes, and in [12] the coordinates were used for mesh deformation. Moreover, in [12] the construction was carried out over arbitrary curves and surfaces, not just polygons and polyhedra. Further work on mean value coordinates and related topics can be found in [1, 4, 5, 11, 13, 15, 17, 22].

The purpose of this paper is to study and further develop mean value interpolation over arbitrary curves in the plane, as proposed by Ju, Schaefer, and Warren [12]. There are two main contributions. The first is the derivation of sufficient conditions on the shape of the boundary that guarantee the interpolation property: conditions that ensure that the mean value interpolant really is an interpolant. This has only previously been shown for polygonal curves with piecewise linear data, in [10]. The second is the construction of a Hermite interpolant, matching values
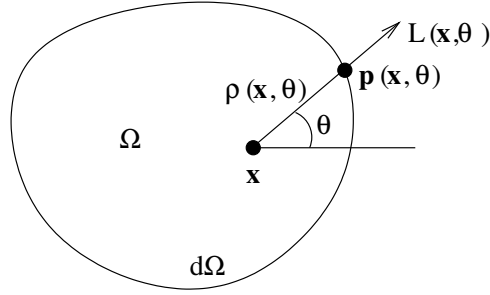
Figure 1: A convex domain.

and normal derivatives of a given function on the boundary. The Hermite interpolant is constructed from a weight function and two Lagrange interpolants, and requires finding their normal derivatives.

We complete the paper with applications to smooth mappings and the web-spline method for solving PDE's.

2 Lagrange interpolation

2.1 Interpolation on convex domains

Let $\Omega \subset \mathbb{R}^2$ be open, bounded and convex. We start with the convexity assumption because the definitions and analysis are easier. However, we make no assumption about the smoothness of the boundary $\partial\Omega$, nor do we demand strict convexity: three points in $\partial\Omega$ can be collinear. Thus we allow Ω to be a convex polygon as well as a circle, ellipse, and so on. For any point $\mathbf{x} = (x_1, x_2)$ in Ω and any angle θ let $L(\mathbf{x}, \theta)$ denote the semi-infinite line that starts at $\mathbf{x}$ and whose angle from the x_1-axis is θ, let $\mathbf{p}(\mathbf{x}, \theta)$ denote the unique point of intersection between $L(\mathbf{x}, \theta)$ and $\partial\Omega$, and let $\rho(\mathbf{x}, \theta)$ be the Euclidean distance $\rho(\mathbf{x}, \theta) = \|\mathbf{p}(\mathbf{x}, \theta) - \mathbf{x}\|$; see Figure 1. The intersection point $\mathbf{p}(\mathbf{x}, \theta)$ depends on the curve $\partial\Omega$, and sometimes it will help to indicate this by writing $\mathbf{p}(\mathbf{x}, \theta; \partial\Omega)$. In general, $\mathbf{p}(\mathbf{x}, \theta; C)$ will denote the intersection (assumed unique) between $L(\mathbf{x}, \theta)$ and any planar curve C and $\rho(\mathbf{x}, \theta; C)$ the corresponding distance.

Given some continuous function $f : \partial\Omega \to \mathbb{R}$, our goal is to define a function $g : \Omega \to \mathbb{R}$ that interpolates f. To do this, for each $\mathbf{x} \in \Omega$, we define $g(\mathbf{x})$ by the following property. If $F : \overline{\Omega} \to \mathbb{R}$ is the linear radial polynomial, linear along each line segment $[\mathbf{x}, \mathbf{y}]$, $\mathbf{y} \in \partial\Omega$, with $F(\mathbf{x}) = g(\mathbf{x})$ and $F(\mathbf{y}) = f(\mathbf{y})$, then F should satisfy the mean value property

$$F(\mathbf{x}) = \frac{1}{2\pi r} \int_\Gamma F(\mathbf{z}) \, d\mathbf{z}, \tag{1}$$

where Γ is any circle in Ω with centre $\mathbf{x}$, and r is its radius. To find $g(\mathbf{x})$, we write (1) as

$$g(\mathbf{x}) = \frac{1}{2\pi} \int_0^{2\pi} F\big(\mathbf{x} + r(\cos\theta, \sin\theta)\big) \, d\theta, \tag{2}$$
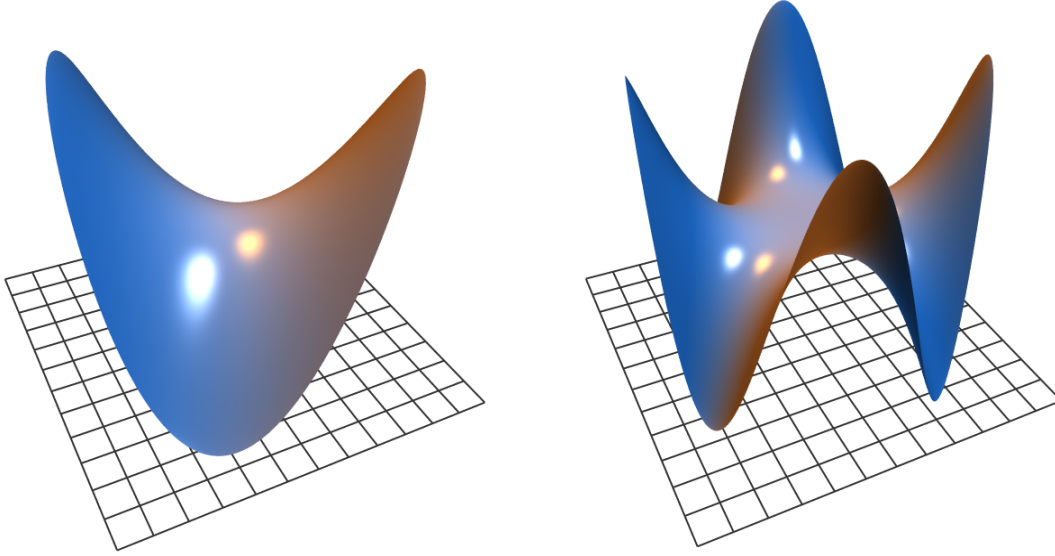
2

Figure 2: Mean value interpolants.

and since
$$F\big(\mathbf{x} + r(\cos\theta, \sin\theta)\big) = \frac{\rho(\mathbf{x}, \theta) - r}{\rho(\mathbf{x}, \theta)} g(\mathbf{x}) + \frac{r}{\rho(\mathbf{x}, \theta)} f(\mathbf{p}(\mathbf{x}, \theta)), \tag{3}$$

equation (2) reduces to
$$\int_0^{2\pi} \frac{f(\mathbf{p}(\mathbf{x}, \theta)) - g(\mathbf{x})}{\rho(\mathbf{x}, \theta)} \, d\theta = 0,$$

whose unique solution is
$$g(\mathbf{x}) = \int_0^{2\pi} \frac{f(\mathbf{p}(\mathbf{x}, \theta))}{\rho(\mathbf{x}, \theta)} \, d\theta \bigg/ \phi(\mathbf{x}), \qquad \phi(\mathbf{x}) = \int_0^{2\pi} \frac{1}{\rho(\mathbf{x}, \theta)} \, d\theta. \tag{4}$$

Equation (4) expresses $g(\mathbf{x})$ as a weighted average of the values of f around Ω. We will show later that under reasonable conditions on $\partial\Omega$, g interpolates f, i.e., that g extends continuously to the boundary $\partial\Omega$ and equals f there. Thus, since F satisfies the mean value property (1) at $\mathbf{x}$, we call g the mean value interpolant to f. The interpolant g itself does not satisfy the mean value theorem and is not in general a harmonic function. But in the spirit of [7], we can view it as 'pseudo-harmonic' as it shares some of the qualitative behaviour of harmonic functions, such as the maximum principle. Also, similar to harmonic functions, the operator I, defined by $g = I(f)$, has linear precision: if $f : \mathbb{R}^2 \to \mathbb{R}$ is any linear function, $f(x_1, x_2) = ax_1 + bx_2 + c$, then $I(f) = f$ in Ω. This follows from the fact that, if f is linear and we let $g(\mathbf{x}) = f(\mathbf{x})$, then $F = f$, and so F is linear and therefore trivially satisfies (1). Figure 2 shows two examples of mean value interpolants on a circular domain.

2.2 Interpolation on convex polygons

The construction of the mean value interpolant g was carried out in [3] in the special case that Ω is a polygon and that f is linear along each edge of the polygon. In this case g is a convex combination of the values of f at the vertices of the polygon. To see this we prove

Lemma 1 *Let $e = [\mathbf{p}_0, \mathbf{p}_1]$ be a line segment and let $f : e \to \mathbb{R}$ be any linear function. Let $\mathbf{x}$ be any point in the open half-plane lying to the left of the vector $\mathbf{p}_1 - \mathbf{p}_0$. Let $\theta_0 < \theta_1$ be the two angles such that $\mathbf{p}(\mathbf{x}, \theta_i; e) = \mathbf{p}_i$, $i = 0, 1$, and let $\rho_i = \|\mathbf{p}_i - \mathbf{x}\|$. Then*

$$\int_{\theta_0}^{\theta_1} \frac{f(\mathbf{p}(\mathbf{x}, \theta; e))}{\rho(\mathbf{x}, \theta; e)} \, d\theta = \left(\frac{f(\mathbf{p}_0)}{\rho_0} + \frac{f(\mathbf{p}_1)}{\rho_1} \right) \tan \left(\frac{\theta_1 - \theta_0}{2} \right). \tag{5}$$

Proof. Similar to the approach of [3], since f is linear, we have with $\mathbf{p} = \mathbf{p}(\mathbf{x}, \theta; e)$,

$$f(\mathbf{p}) = \frac{A_1}{A} f(\mathbf{p}_0) + \frac{A_0}{A} f(\mathbf{p}_1), \tag{6}$$

with A_0, A_1, A the triangle areas $A_0 = A([\mathbf{p}_0, \mathbf{x}, \mathbf{p}])$, $A_1 = A([\mathbf{p}, \mathbf{x}, \mathbf{p}_1])$, $A = A([\mathbf{p}_0, \mathbf{x}, \mathbf{p}_1])$. Letting $\rho = \rho(\mathbf{x}, \theta; e)$, by the sine rule,

$$\frac{A_0}{A} = \frac{\sin(\theta - \theta_0)\rho}{\sin(\theta_1 - \theta_0)\rho_1}, \qquad \frac{A_1}{A} = \frac{\sin(\theta_1 - \theta)\rho}{\sin(\theta_1 - \theta_0)\rho_0},$$

and putting these into (6), dividing by ρ, and integrating from θ_0 to θ_1 gives (5). $\qquad \square$

Since the function $f \equiv 1$ is linear, the lemma also shows that

$$\int_{\theta_0}^{\theta_1} \frac{1}{\rho(\mathbf{x}, \theta; e)} \, d\theta = \left(\frac{1}{\rho_0} + \frac{1}{\rho_1} \right) \tan \left(\frac{\theta_1 - \theta_0}{2} \right).$$

Together with (5), this implies that, if Ω is a convex polygon with vertices $\mathbf{p}_0, \mathbf{p}_1, \ldots, \mathbf{p}_{n-1}$, and, indexing modulo n, if f is linear on each edge $[\mathbf{p}_i, \mathbf{p}_{i+1}]$, then g in (4) reduces to

$$g(\mathbf{x}) = \sum_{i=0}^{n-1} w_i(\mathbf{x}) f(\mathbf{p}_i) \Big/ \phi(\mathbf{x}), \qquad \phi(\mathbf{x}) = \sum_{i=0}^{n-1} w_i(\mathbf{x}), \tag{7}$$

where

$$w_i(\mathbf{x}) := \frac{\tan(\alpha_{i-1}(\mathbf{x})/2) + \tan(\alpha_i(\mathbf{x})/2)}{\rho_i(\mathbf{x})}, \tag{8}$$

and $\rho_i(\mathbf{x}) = \|\mathbf{p}_i - \mathbf{x}\|$ and $\alpha_i(\mathbf{x})$ is the angle at $\mathbf{x}$ of the triangle with vertices $\mathbf{x}, \mathbf{p}_i, \mathbf{p}_{i+1}$. The functions

$$\lambda_i(\mathbf{x}) := w_i(\mathbf{x}) \Big/ \sum_{j=0}^{n-1} w_j(\mathbf{x}),$$

were called mean value coordinates in [3]. By the linear precision property of I, since both $f(\mathbf{x}) = x_1$ and $f(\mathbf{x}) = x_2$ are linear, we have

$$\mathbf{x} = \sum_{i=0}^{n-1} \lambda_i(\mathbf{x})\mathbf{p}_i,$$

which expresses $\mathbf{x}$ as a convex combination of the vertices $\mathbf{p}_i$. Thus, the coordinates λ_i are a generalization of barycentric coordinates.

2.3 The boundary integral formula

It is not clear from the formula (4) how to differentiate g. Ju, Schaefer, and Warren [12] noticed however that if a parametric representation of $\partial\Omega$ is available, the two integrals in (4) can be converted to integrals over the parameter of the curve. Let $\mathbf{c} : [a, b] \rightarrow \mathbb{R}^2$, with $\mathbf{c}(b) = \mathbf{c}(a)$, be some parametric representation of $\partial\Omega$, oriented anti-clockwise with respect to increasing parameter values. If $\mathbf{c}(t) = (c_1(t), c_2(t)) = \mathbf{p}(\mathbf{x}, \theta)$, then θ is given by

$$\theta = \arctan\left(\frac{c_2(t) - x_2}{c_1(t) - x_1}\right), \tag{9}$$

and differentiating this with respect to t gives

$$\frac{d\theta}{dt} = \frac{(c_1(t) - x_1)c_2'(t) - (c_2(t) - x_2)c_1'(t)}{(c_1(t) - x_1)^2 + (c_2(t) - x_2)^2} = \frac{(\mathbf{c}(t) - \mathbf{x}) \times \mathbf{c}'(t)}{\|\mathbf{c}(t) - \mathbf{x}\|^2}, \tag{10}$$

where $\times$ denotes the cross product in $\mathbb{R}^2$, i.e, $\mathbf{a} \times \mathbf{b} := a_1 b_2 - a_2 b_1$. Using (10) to change the integration variable in (4) yields the boundary integral representation (c.f. [12]),

$$g(\mathbf{x}) = \int_a^b w(\mathbf{x}, t) f(\mathbf{c}(t)) \, dt \Big/ \phi(\mathbf{x}), \qquad \phi(\mathbf{x}) = \int_a^b w(\mathbf{x}, t) \, dt, \tag{11}$$

where

$$w(\mathbf{x}, t) = \frac{(\mathbf{c}(t) - \mathbf{x}) \times \mathbf{c}'(t)}{\|\mathbf{c}(t) - \mathbf{x}\|^3}. \tag{12}$$

It is now clear that we can take as many partial derivatives of g as we like by differentiating under the integral sign in (11). Thus we see that g is in $C^\infty(\Omega)$. The boundary integral formula is also important because it provides a way of numerically computing the value of g at a point $\mathbf{x}$ by sampling the curve $\mathbf{c}$ and its first derivative $\mathbf{c}'$ and applying some standard quadrature rule to the two integrals in (11). A simple alternative evaluation method that only requires evaluating $\mathbf{c}$ itself is to make a polygonal approximation to $\mathbf{c}$ and apply (7). The third alternative of using the original angle formula (4) and sampling the angles between 0 and 2π requires computing the intersection points $\mathbf{p}(\mathbf{x}, \theta)$.

The numerator in w can also be written as the scalar product of $(\mathbf{c}(t) - \mathbf{x})$ and $\mathrm{rot}(\mathbf{c}'(t)) = (c_2'(t), -c_1'(t))$, the rotation of $\mathbf{c}'(t)$ through an angle of $-\pi/2$. Then, since the outward normal to the curve $\mathbf{c}$ is $\mathrm{rot}(\mathbf{c}'(t))/\|\mathbf{c}'(t)\|$, another way of representing g is in terms of flux integrals:

$$g(\mathbf{x}) = \int_{\partial\Omega} f(\mathbf{y})\mathbf{F}(\mathbf{y}) \cdot \mathbf{N}(\mathbf{y}) \, d\mathbf{y} \Big/ \phi(\mathbf{x}), \qquad \phi(\mathbf{x}) = \int_{\partial\Omega} \mathbf{F}(\mathbf{y}) \cdot \mathbf{N}(\mathbf{y}) \, d\mathbf{y},$$

where $\mathbf{F}$ is the vector field

$$\mathbf{F}(\mathbf{y}) = \frac{\mathbf{y} - \mathbf{x}}{\|\mathbf{y} - \mathbf{x}\|^3},$$

and $\mathbf{N}(\mathbf{y})$ is the outward unit normal at $\mathbf{y}$ and $d\mathbf{y}$ denotes the element of arc length of $\partial\Omega$. The Gauss theorem could then be applied to these expressions to give further formulas for g and ϕ. Recently, Lee [16] has studied more general formulas of this type.

2.4 Non-convex domains

We now turn our attention to the case that Ω is an arbitrary connected open domain in $\mathbb{R}^2$, not necessarily convex. In the case that Ω is a polygon, it was shown in [10] that the mean value interpolant g defined by (7–8) has a natural extension to non-convex polygons if we simply allow $\alpha_i(\mathbf{x})$ in (8) to be a signed angle: negative when $\mathbf{x}$ lies to the right of the vector $\mathbf{p}_{i+1} - \mathbf{p}_i$. The main point is that ϕ continues to be strictly positive in Ω so that g is well defined.

To deal with arbitrary (non-polygonal) domains, suppose initially that Ω is simply-connected, i.e., has no holes, in which case its boundary can be represented as a single parametric curve $\mathbf{c} : [a, b] \to \mathbb{R}^2$, with $\mathbf{c}(b) = \mathbf{c}(a)$, oriented anti-clockwise. Then, similar to the construction in [12], we define g in this more general setting by the boundary integral (11). Note that for arbitrary $\mathbf{x} \in \Omega$ the quantity $w(\mathbf{x}, t)$ may change sign several times as t varies.

We can also express g in this general setting using angle integrals. Recall that an intersection point of two smooth planar curves is said to be *transversal* if the curves have distinct tangents at that point. We call θ a *transversal angle* with respect to $\mathbf{x}$ if all the intersections between $L(\mathbf{x}, \theta)$ and $\partial\Omega$ are transversal. For example, in Figure 3a all angles at $\mathbf{x}$ are transversal except for θ_1 and θ_2. We make the assumption that $\partial\Omega$ is such that there is a finite number of non-transversal angles at each $\mathbf{x} \in \Omega$. If θ is a transversal angle, let $n(\mathbf{x}, \theta)$ be the number of intersections of $L(\mathbf{x}, \theta)$ with $\partial\Omega$ which will be an odd number, assumed finite, and let $\mathbf{p}_j(\mathbf{x}, \theta)$, $j = 1, 2, \ldots, n(\mathbf{x}, \theta)$, be the points of intersection, ordered so that their distances $\rho_j(\mathbf{x}, \theta) = \|\mathbf{p}_j(\mathbf{x}, \theta) - \mathbf{x}\|$ are increasing,

$$\rho_1(\mathbf{x}, \theta) < \rho_2(\mathbf{x}, \theta) < \cdots < \rho_{n(\mathbf{x},\theta)}(\mathbf{x}, \theta). \tag{13}$$

For example, for $\theta \in (\theta_1, \theta_2)$ in Figure 3a, there are three such intersections, shown in Figure 3b.

Now for fixed $\mathbf{x} \in \Omega$, let

$$S_+ = \{t \in [a, b] : w(\mathbf{x}, t) > 0\} \qquad \text{and} \qquad S_- = \{t \in [a, b] : w(\mathbf{x}, t) < 0\},$$

and observe that both integrals in (11) reduce to integrals over S_+ and S_-. Moreover, the sets S_+ and S_- are unions of intervals, and thus the integrals in (11) are sums of integrals, one integral
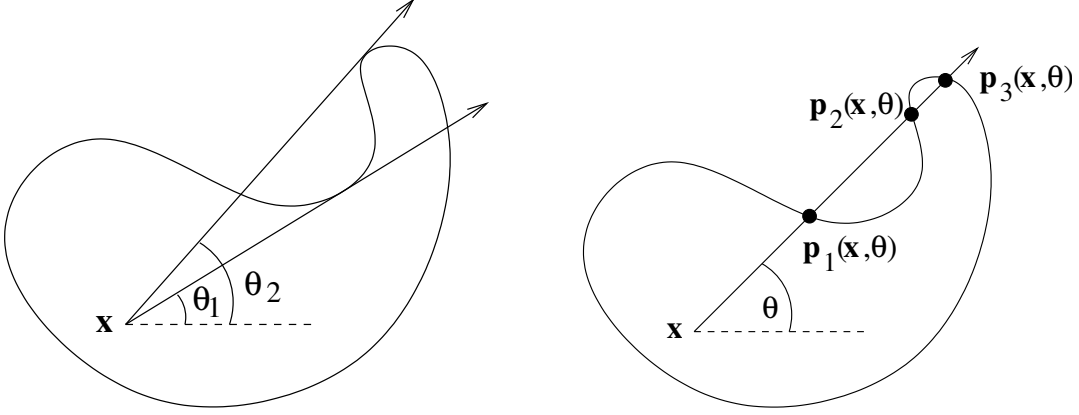
Figure 3: (a) Example with two non-transversal angles and (b) an angle with three intersections.

for each interval, and $w(\mathbf{x}, \cdot)$ has constant sign in each interval. By changing the variable of integration for each interval from t to θ, using (10), it follows that g can be expressed as

$$g(\mathbf{x}) = \int_0^{2\pi} \sum_{j=1}^{n(\mathbf{x},\theta)} \frac{(-1)^{j-1}}{\rho_j(\mathbf{x},\theta)} f(\mathbf{p}_j(\mathbf{x},\theta)) \, d\theta \bigg/ \phi(\mathbf{x}), \qquad \phi(\mathbf{x}) = \int_0^{2\pi} \sum_{j=1}^{n(\mathbf{x},\theta)} \frac{(-1)^{j-1}}{\rho_j(\mathbf{x},\theta)} \, d\theta. \quad (14)$$

Here, if θ is not a transversal angle, we set $n(\mathbf{x},\theta) = 0$. We now use (14) to deduce the positivity of ϕ and therefore the validity of g in the non-convex case.

Theorem 1 *For all* $\mathbf{x} \in \Omega$, $\phi(\mathbf{x}) > 0$.

Proof. The argument is similar to the polygonal case treated in [10]. Since the sequence of distances in (13) is increasing, if $n(\mathbf{x}, \theta) \geq 3$,

$$\frac{1}{\rho_{2j-1}(\mathbf{x},\theta)} - \frac{1}{\rho_{2j}(\mathbf{x},\theta)} > 0, \qquad j = 1, 2, \dots, (n(\mathbf{x},\theta) - 1)/2,$$

and so (14) implies

$$\phi(\mathbf{x}) \geq \int_0^{2\pi} \frac{1}{\rho_{n(\mathbf{x},\theta)}(\mathbf{x},\theta)} \, d\theta > 0.$$

$\square$

2.5 Bounds on ϕ

Having shown that g, given by either (11) or (14), is well-defined for non-convex domains, our next goal is to show that g interpolates the boundary data f under reasonable conditions on the shape of the boundary. A crucial step in this is to study the behaviour of ϕ near the boundary. In this section we show that ϕ behaves like the reciprocal of the distance function $\mathrm{d}(\mathbf{x}, \partial\Omega)$, the minimum distance between a point $\mathbf{x} \in \Omega$ and the set $\partial\Omega$. First we derive an upper bound.

Theorem 2 *For any* $\mathbf{x} \in \Omega$,

$$\phi(\mathbf{x}) \leq \frac{2\pi}{d(\mathbf{x}, \partial\Omega)}. \tag{15}$$

Proof. If $n(\mathbf{x}, \theta) \geq 3$ in equation (13), then

$$\frac{-1}{\rho_{2j}(\mathbf{x}, \theta)} + \frac{1}{\rho_{2j+1}(\mathbf{x}, \theta)} < 0, \qquad j = 1, 2, \ldots, (n(\mathbf{x}, \theta) - 1)/2,$$

and so

$$\phi(\mathbf{x}) \leq \int_0^{2\pi} \frac{1}{\rho_1(\mathbf{x}, \theta)} \, d\theta \leq \int_0^{2\pi} \frac{1}{d(\mathbf{x}, \partial\Omega)} \, d\theta.$$

$\square$

To derive a lower bound for ϕ, we make some assumptions about $\partial\Omega$ in terms of its medial axis [2]. Observe that $\partial\Omega$ divides $\mathbb{R}^2$ into two open and disjoint sets, the set Ω itself, and its complement Ω^C. The interior / exterior medial axis $M_I \subset \mathbb{R}^2$ / $M_E \subset \mathbb{R}^2$ of $\partial\Omega$ is the set of all points in Ω / Ω^C whose minimal distance to $\partial\Omega$ is attained at least twice. For any set $M \subset \mathbb{R}^2$, we let

$$d(M, \partial\Omega) = \inf_{\mathbf{y} \in M} d(\mathbf{y}, \partial\Omega),$$

and to derive a lower bound, we will make the assumption that $d(M_E, \partial\Omega) > 0$. Note that this condition holds for convex curves because in the convex case, $M_E = \emptyset$ and $d(M_E, \partial\Omega) = \infty$. We will also make use of the diameter of Ω,

$$\mathrm{diam}(\Omega) = \sup_{\mathbf{y}_1, \mathbf{y}_2 \in \partial\Omega} \|\mathbf{y}_1 - \mathbf{y}_2\|.$$

Theorem 3 *If* $d = d(M_E, \partial\Omega) > 0$, *there is a constant* $C > 0$ *such that for* $\mathbf{x} \in \Omega$,

$$\phi(\mathbf{x}) \geq \frac{C}{d(\mathbf{x}, \partial\Omega)}. \tag{16}$$

With β *the ratio* $\beta = D/d$, *where* $D = \mathrm{diam}(\Omega)$, *we can take*

$$C = \frac{2}{(1 + \beta)(1 + \beta + \sqrt{\beta^2 + 2\beta})}.$$

Note that $C \leq 2$ and if Ω is convex then $\beta = 0$ and $C = 2$. On the other hand, if d is small relative to D, then C will be small.

Proof. Let $\mathbf{y}$ be some boundary point such that $d(\mathbf{x}, \partial\Omega) = \|\mathbf{y} - \mathbf{x}\|$, and let $\delta = \|\mathbf{y} - \mathbf{x}\|$ and let $\theta_{\mathbf{y}} \in [0, 2\pi)$ be the angle such that $L(\mathbf{x}, \theta_{\mathbf{y}})$ intersects $\mathbf{y}$. Then the open disc $B_1 = B(\mathbf{x}, \delta)$ is contained in Ω. By the assumption that $d > 0$, let $\mathbf{x}_C$ be the point in Ω^C on the line $L(\mathbf{x}, \theta_{\mathbf{y}})$ whose distance from $\mathbf{y}$ is d; see Figure 4. Then the open disc $B_2 = B(\mathbf{x}_C, d)$ is contained in Ω^C. Let α_1, α_2, with $\alpha_1 < \theta_{\mathbf{y}} < \alpha_2$, be the two angles such that the lines $L(\mathbf{x}, \alpha_1)$ and $L(\mathbf{x}, \alpha_2)$ are
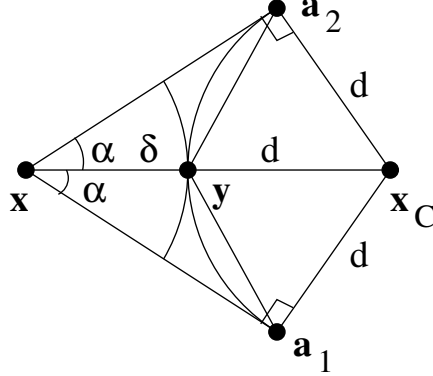
Figure 4: Lines in proof of Theorem 3.

tangential to ∂B_2, and let $\mathbf{a}_i$, $i = 1, 2$, be the point where $L(\mathbf{x}, \alpha_i)$ touches ∂B_2. Let $\mathbf{q}_1$ be the polygon consisting of the two line segments $[\mathbf{a}_1, \mathbf{y}]$ and $[\mathbf{y}, \mathbf{a}_2]$, and $\mathbf{q}_2$ the polygon consisting of $[\mathbf{a}_1, \mathbf{x}_C]$ and $[\mathbf{x}_C, \mathbf{a}_2]$.

Let θ be any transversal angle in (α_1, α_2). Then there is some odd number k, say with $k \leq n(\mathbf{x}, \theta)$, such that the intersection points $\mathbf{p}_1(\mathbf{x}, \theta), \ldots, \mathbf{p}_k(\mathbf{x}, \theta)$ lie between B_1 and B_2 while the remaining ones $\mathbf{p}_{k+1}(\mathbf{x}, \theta), \ldots, \mathbf{p}_{n(\mathbf{x},\theta)}(\mathbf{x}, \theta)$ lie beyond B_2. Then, similar to the proof of Theorem 1, if $k = n(\mathbf{x}, \theta)$, the sum in ϕ in (14) satisfies the inequality

$$\sum_{j=1}^{n(\mathbf{x},\theta)} \frac{(-1)^{j-1}}{\rho_j(\mathbf{x}, \theta)} \geq \frac{1}{\rho_k(\mathbf{x}, \theta)},$$

while, if $k < n(\mathbf{x}, \theta)$, it satisfies

$$\sum_{j=1}^{n(\mathbf{x},\theta)} \frac{(-1)^{j-1}}{\rho_j(\mathbf{x}, \theta)} \geq \frac{1}{\rho_k(\mathbf{x}, \theta)} - \frac{1}{\rho_{k+1}(\mathbf{x}, \theta)}.$$

Consequently, in either case

$$\sum_{j=1}^{n(\mathbf{x},\theta)} \frac{(-1)^{j-1}}{\rho_j(\mathbf{x}, \theta)} \geq \frac{1}{\rho(\mathbf{x}, \theta; \mathbf{q}_1)} - \frac{1}{\rho(\mathbf{x}, \theta; \mathbf{q}_2)},$$

and therefore, from (14),

$$\phi(\mathbf{x}) \geq \int_{\alpha_1}^{\alpha_2} \left(\frac{1}{\rho(\mathbf{x}, \theta; \mathbf{q}_1)} - \frac{1}{\rho(\mathbf{x}, \theta; \mathbf{q}_2)} \right) d\theta.$$

We now use the explicit formula from Lemma 1, and setting $\alpha = (\alpha_2 - \alpha_1)/2$, we find

$$\phi(\mathbf{x}) \geq 2 \left(\frac{1}{\|\mathbf{a}_1 - \mathbf{x}\|} + \frac{1}{\|\mathbf{y} - \mathbf{x}\|} \right) \tan(\alpha/2) - 2 \left(\frac{1}{\|\mathbf{a}_1 - \mathbf{x}\|} + \frac{1}{\|\mathbf{x}_C - \mathbf{x}\|} \right) \tan(\alpha/2)$$

9

$$= 2\left(\frac{1}{\delta} - \frac{1}{\delta + d}\right)\tan(\alpha/2) = \frac{2d}{\delta(\delta + d)}\tan(\alpha/2).$$

Moreover, since

$$\tan(\alpha/2) = \frac{1 - \cos\alpha}{\sin\alpha}, \qquad \sin\alpha = \frac{d}{\delta + d}, \qquad \cos\alpha = \frac{\sqrt{(\delta + d)^2 - d^2}}{\delta + d},$$

we have

$$\tan(\alpha/2) = \frac{d}{\delta + d + \sqrt{(\delta + d)^2 - d^2}},$$

and therefore

$$\phi(\mathbf{x}) \geq \frac{1}{\delta}\left(\frac{2d}{\delta + d}\right)\left(\frac{d}{\delta + d + \sqrt{\delta^2 + 2\delta d}}\right). \tag{17}$$

Since $\delta \leq D$, this implies

$$\phi(\mathbf{x}) \geq \frac{1}{\delta}\left(\frac{2d}{D + d}\right)\left(\frac{d}{D + d + \sqrt{D^2 + 2Dd}}\right).$$

and, putting $D = \beta d$ and cancelling the d's, proves the theorem. $\qquad\square$

2.6 Proof of interpolation

We can now prove that g really interpolates f under the medial axis condition of Theorem 3. We also make the mild assumption that

$$N := \sup_{\mathbf{x}\in\Omega}\ \sup_{\theta\in T(\mathbf{x})}\ n(\mathbf{x}, \theta) < \infty, \tag{18}$$

where $T(\mathbf{x})$ is the subset of $[0, 2\pi)$ of those angles that are transversal with respect to $\mathbf{x}$. Note that this holds for convex Ω, in which case $N = 1$.

Theorem 4 *If f is continuous on $\partial\Omega$ and $\mathrm{d}(M_E, \partial\Omega) > 0$, then g interpolates f.*

Proof. Let $\mathbf{c}(s)$ be any boundary point and observe that for $\mathbf{x} \in \Omega$,

$$g(\mathbf{x}) - f(\mathbf{c}(s)) = \frac{1}{\phi(\mathbf{x})}\int_a^b w(\mathbf{x}, t)\big(f(\mathbf{c}(t)) - f(\mathbf{c}(s))\big)\, dt. \tag{19}$$

We will choose some small $\gamma > 0$ and split the integral into two parts, $\int_a^b = \int_I + \int_J$, where $I = [s - \gamma, s + \gamma]$ and $J = [a, b] \setminus I$. Then, with $M := \sup_{\mathbf{y}\in\partial\Omega}|f(\mathbf{y})|$,

$$|g(\mathbf{x}) - f(\mathbf{c}(s))| \leq \max_{t\in I}|f(\mathbf{c}(t)) - f(\mathbf{c}(s))|\frac{1}{\phi(\mathbf{x})}\int_I |w(\mathbf{x}, t)|\, dt + 2M\frac{1}{\phi(\mathbf{x})}\int_J |w(\mathbf{x}, t)|\, dt.$$

Considering the first term on the right hand side, note that

$$\frac{1}{\phi(\mathbf{x})} \int_I |w(\mathbf{x}, t)| \, dt \leq \frac{1}{\phi(\mathbf{x})} \int_a^b |w(\mathbf{x}, t)| \, dt =: R,$$

which we will bound above. The argument used to derive (14) also shows that

$$\int_a^b |w(\mathbf{x}, t)| \, dt = \int_0^{2\pi} \sum_{j=1}^{n(\mathbf{x},\theta)} \frac{1}{\rho_j(\mathbf{x}, \theta)} \, d\theta,$$

and so

$$\int_a^b |w(\mathbf{x}, t)| \, dt = \phi(\mathbf{x}) + 2 \int_0^{2\pi} \sum_{j=1}^{(n(\mathbf{x},\theta)-1)/2} \frac{1}{\rho_{2j}(\mathbf{x}, \theta)} \, d\theta \leq \phi(\mathbf{x}) + \frac{2(N-1)\pi}{\mathrm{d}(\mathbf{x}, \partial\Omega)},$$

with N as in (18). Dividing by $\phi(\mathbf{x})$ and applying the lower bound (16) to $\phi(\mathbf{x})$, then leads to

$$R \leq 1 + \frac{2(N-1)\pi}{\phi(\mathbf{x})\mathrm{d}(\mathbf{x}, \partial\Omega)} \leq 1 + \frac{2(N-1)\pi}{C},$$

which is independent of $\mathbf{x}$. Note that when Ω is convex, $N = 1$ and $R = 1$.

Let $\epsilon > 0$. We must show that there is some $\delta > 0$ such that if $\mathbf{x} \in \Omega$ and $\|\mathbf{x} - \mathbf{c}(s)\| \leq \delta$ then $|g(\mathbf{x}) - f(\mathbf{c}(s))| < \epsilon$. Since $f \circ \mathbf{c}$ is continuous at $t = s$, we can choose $\gamma > 0$ such that $|f(\mathbf{c}(t)) - f(\mathbf{c}(s))| < (\epsilon/2)/(1 + 2(N-1)\pi/C)$ for $t \in I$. Then

$$|g(\mathbf{x}) - f(\mathbf{c}(s))| < \frac{\epsilon}{2} + 2M \frac{1}{\phi(\mathbf{x})} \int_J |w(\mathbf{x}, t)| \, dt. \tag{20}$$

Finally, since

$$\lim_{\mathbf{x} \to \mathbf{c}(s)} \int_J |w(\mathbf{x}, t)| \, dt = \int_J |w(\mathbf{c}(s), t)| \, dt < \infty, \qquad \text{and} \qquad \lim_{\mathbf{x} \to \mathbf{c}(s)} \phi(\mathbf{x}) = \infty,$$

it follows that there is some $\delta > 0$ such that if $\mathbf{x} \in \Omega$ and $\|\mathbf{x} - \mathbf{c}(s)\| \leq \delta$ then

$$\frac{1}{\phi(\mathbf{x})} \int_J |w(\mathbf{x}, t)| \, dt < \frac{\epsilon}{4M},$$

in which case $|g(\mathbf{x}) - f(\mathbf{c}(s))| < \epsilon$. □

3   Differentiation

In some applications we might need to compute derivatives of g. Let $\boldsymbol{\alpha} = (\alpha_1, \alpha_2)$ be a multi-index, and let $D_{\boldsymbol{\alpha}} = \partial^{\alpha_1 + \alpha_2}/(\partial^{\alpha_1} x_1 \partial^{\alpha_2} x_2)$. We start by expressing g in (11) as $g(\mathbf{x}) = \sigma(\mathbf{x})/\phi(\mathbf{x})$, where

$$\sigma(\mathbf{x}) = \int_a^b w(\mathbf{x}, t) f(\mathbf{c}(t)) \, dt,$$

and we reduce the task of computing derivatives of g to that of computing derivatives of σ and ϕ, which are given by

$$D_{\boldsymbol{\alpha}}\sigma(\mathbf{x}) = \int_a^b D_{\boldsymbol{\alpha}}w(\mathbf{x},t)f(\mathbf{c}(t))\,dt, \quad \text{and} \quad D_{\boldsymbol{\alpha}}\phi(\mathbf{x}) = \int_a^b D_{\boldsymbol{\alpha}}w(\mathbf{x},t)\,dt,$$

with $D_{\boldsymbol{\alpha}}$ operating with respect to the $\mathbf{x}$ variable. Letting $\binom{\boldsymbol{\alpha}}{\boldsymbol{\beta}} = \binom{\alpha_1}{\beta_1}\binom{\alpha_2}{\beta_2}$, and defining $\boldsymbol{\beta} \leq \boldsymbol{\alpha}$ to mean that $\beta_i \leq \alpha_i$ for both $i = 1, 2$, and $\boldsymbol{\beta} < \boldsymbol{\alpha}$ to mean that $\boldsymbol{\beta} \leq \boldsymbol{\alpha}$ and $\boldsymbol{\alpha} \neq \boldsymbol{\beta}$, we take the $D_{\boldsymbol{\alpha}}$ derivative of the equation $\phi(\mathbf{x})g(\mathbf{x}) = \sigma(\mathbf{x})$, and the Leibniz rule gives

$$\sum_{0 \leq \boldsymbol{\beta} \leq \boldsymbol{\alpha}} \binom{\boldsymbol{\alpha}}{\boldsymbol{\beta}} D_{\boldsymbol{\beta}}\phi(\mathbf{x})D_{\boldsymbol{\alpha}-\boldsymbol{\beta}}g(\mathbf{x}) = D_{\boldsymbol{\alpha}}\sigma(\mathbf{x}),$$

and by rearranging this in the form

$$D_{\boldsymbol{\alpha}}g(\mathbf{x}) = \frac{1}{\phi(\mathbf{x})}\left(D_{\boldsymbol{\alpha}}\sigma(\mathbf{x}) - \sum_{0 < \boldsymbol{\beta} \leq \boldsymbol{\alpha}} \binom{\boldsymbol{\alpha}}{\boldsymbol{\beta}} D_{\boldsymbol{\beta}}\phi(\mathbf{x})D_{\boldsymbol{\alpha}-\boldsymbol{\beta}}g(\mathbf{x})\right), \tag{21}$$

we obtain a rule for computing all partial derivatives of g recursively from those of σ and ϕ. Letting

$$\mathbf{d} = \mathbf{d}(\mathbf{x},t) = \mathbf{c}(t) - \mathbf{x}, \qquad r = r(\mathbf{x},t) = \|\mathbf{d}(\mathbf{x},t)\|, \tag{22}$$

so that $r^3 w = \mathbf{d} \times \mathbf{c}'$, an approach similar to the derivation of (21) gives

$$D_{\boldsymbol{\alpha}}w = \frac{1}{r^3}\left(D_{\boldsymbol{\alpha}}(\mathbf{d} \times \mathbf{c}') - \sum_{0 < \boldsymbol{\beta} \leq \boldsymbol{\alpha}} D_{\boldsymbol{\beta}}(r^3)D_{\boldsymbol{\alpha}-\boldsymbol{\beta}}w\right), \tag{23}$$

a rule to compute the partial derivatives of w recursively. Since it is easy to differentiate r^2, we can use the Leibniz rule to differentiate r^3:

$$D_{\boldsymbol{\alpha}}(r^3) = D_{\boldsymbol{\alpha}}(r^2 r) = \sum_{0 \leq \boldsymbol{\beta} \leq \boldsymbol{\alpha}} \binom{\boldsymbol{\alpha}}{\boldsymbol{\beta}} D_{\boldsymbol{\beta}}(r^2)D_{\boldsymbol{\alpha}-\boldsymbol{\beta}}r.$$

By applying the Leibniz rule to r^2, we obtain derivatives of r:

$$D_{\boldsymbol{\alpha}}r = \frac{1}{2r}\left(D_{\boldsymbol{\alpha}}(r^2) - \sum_{0 < \boldsymbol{\beta} < \boldsymbol{\alpha}} \binom{\boldsymbol{\alpha}}{\boldsymbol{\beta}} D_{\boldsymbol{\beta}}r D_{\boldsymbol{\alpha}-\boldsymbol{\beta}}r\right). \tag{24}$$

In the case that $\partial\Omega$ is a polygon, we can differentiate the explicit formula of g in (7), which boils down to differentiating w_i in (8). Similar to (21) we have

$$D_{\boldsymbol{\alpha}}\left(\frac{1}{\rho_i}\right) = -\frac{1}{\rho_i}\sum_{0 < \boldsymbol{\beta} \leq \boldsymbol{\alpha}} \binom{\boldsymbol{\alpha}}{\boldsymbol{\beta}} D_{\boldsymbol{\beta}}\rho_i D_{\boldsymbol{\alpha}-\boldsymbol{\beta}}\left(\frac{1}{\rho_i}\right),$$

and the formula for $D_{\boldsymbol{\alpha}}\rho_i$ is given by (24) with r replaced by ρ_i. Derivatives of $\tan(\alpha_i/2)$ can be found by rewriting it in terms of scalar and cross products of $\mathbf{d}_i(\mathbf{x}) = \mathbf{p}_i - \mathbf{x}$,

$$\tan\left(\frac{\alpha_i}{2}\right) = \frac{\rho_i \rho_{i+1} - \mathbf{d}_i \cdot \mathbf{d}_{i+1}}{\mathbf{d}_i \times \mathbf{d}_{i+1}}.$$

Then, by viewing this as a quotient, we have

$$D_{\boldsymbol{\alpha}} \tan\left(\frac{\alpha_i}{2}\right) = \frac{1}{\mathbf{d}_i \times \mathbf{d}_{i+1}} \left(D_{\boldsymbol{\alpha}}(\rho_i \rho_{i+1} - \mathbf{d}_i \cdot \mathbf{d}_{i+1}) - \sum_{0 < \boldsymbol{\beta} \leq \boldsymbol{\alpha}} D_{\boldsymbol{\beta}}(\mathbf{d}_i \times \mathbf{d}_{i+1}) D_{\boldsymbol{\alpha}-\boldsymbol{\beta}} \tan\left(\frac{\alpha_i}{2}\right) \right).$$

4 Hermite interpolation

We now construct a Hermite interpolant based on mean value interpolation. As we will see, the interpolant is a natural generalization of cubic Hermite interpolation in one variable, and it helps to recall the latter. Given the values and first derivatives of some function $f : \mathbb{R} \to \mathbb{R}$ at the points $x_0 < x_1$, cubic Hermite interpolation consists of finding the unique cubic polynomial p such that

$$p(x_i) = f(x_i) \qquad \text{and} \qquad p'(x_i) = f'(x_i), \qquad i = 0, 1. \tag{25}$$

One way of expressing p is in the form

$$p(x) = g_0(x) + \psi(x)g_1(x), \tag{26}$$

where g_0 is the linear Lagrange interpolant

$$g_0(x) = \frac{x_1 - x}{x_1 - x_0} f(x_0) + \frac{x - x_0}{x_1 - x_0} f(x_1),$$

ψ is the quadratic weight function

$$\psi(x) = \frac{(x - x_0)(x_1 - x)}{x_1 - x_0},$$

and g_1 is another linear Lagrange interpolant,

$$g_1(x) = \frac{x_1 - x}{x_1 - x_0} m_0 + \frac{x - x_0}{x_1 - x_0} m_1,$$

whose data m_0 and m_1 are yet to be determined. To see this, observe that since $\psi(x_i) = 0$, $i = 0, 1$, p in (26) already meets the Lagrange conditions in (25), and since $\psi'(x_i) \neq 0$ for $i = 0, 1$, the derivative conditions in (25) are met by setting

$$m_i = \frac{f'(x_i) - g_0'(x_i)}{\psi'(x_i)}, \qquad i = 0, 1.$$

Now observe that for $x \in (x_0, x_1)$ we can express g_0 and ψ as

$$g_0(x) = \sum_{i=0}^{1} \frac{f(x_i)}{|x_i - x|} \Big/ \sum_{i=0}^{1} \frac{1}{|x_i - x|} \qquad \text{and} \qquad \psi(x) = 1 \Big/ \sum_{i=0}^{1} \frac{1}{|x_i - x|}, \qquad (27)$$

and similarly for g_1. Therefore, by viewing $|x_i - x|$ as the distance from x to the boundary point x_i of the domain (x_0, x_1) we see that the mean value interpolant g in (4) is a generalization of the linear univariate interpolant g_0 to two variables. Similarly, ϕ in (4) generalizes the denominator of ψ above. This suggests a Hermite approach for the curve case. Given the values and inward normal derivative of a function f defined on $\partial\Omega$, we seek a function $p : \overline{\Omega} \to \mathbb{R}$ satisfying

$$p(\mathbf{y}) = f(\mathbf{y}) \qquad \text{and} \qquad \frac{\partial p}{\partial \mathbf{n}}(\mathbf{y}) = \frac{\partial f}{\partial \mathbf{n}}(\mathbf{y}), \qquad \mathbf{y} \in \partial\Omega, \qquad (28)$$

in the form

$$p(\mathbf{x}) = g_0(\mathbf{x}) + \psi(\mathbf{x})g_1(\mathbf{x}), \qquad (29)$$

where g_0 is the Lagrange mean value interpolant to f in (11), ψ is the weight function

$$\psi(\mathbf{x}) = \frac{1}{\phi(\mathbf{x})}, \qquad (30)$$

with ϕ from (11), and g_1 is a second Lagrange mean value interpolant whose data is yet to be decided. Similar to the univariate case, we need to show that $\psi(\mathbf{y}) = 0$ and $\frac{\partial \psi}{\partial \mathbf{n}}(\mathbf{y}) \neq 0$ for $\mathbf{y} \in \partial\Omega$. Then we obtain (28) by setting

$$g_1(\mathbf{y}) = \left(\frac{\partial f}{\partial \mathbf{n}}(\mathbf{y}) - \frac{\partial g_0}{\partial \mathbf{n}}(\mathbf{y}) \right) \Big/ \frac{\partial \psi}{\partial \mathbf{n}}(\mathbf{y}), \qquad \mathbf{y} \in \partial\Omega. \qquad (31)$$

Thus we also need to determine $\frac{\partial \psi}{\partial \mathbf{n}}(\mathbf{y})$ and $\frac{\partial g_0}{\partial \mathbf{n}}(\mathbf{y})$. We treat each of these requirements in turn.

First, observe that Theorems 2 and 3 give the upper and lower bounds

$$\frac{1}{2\pi}\mathrm{d}(\mathbf{x}, \partial\Omega) \leq \psi(\mathbf{x}) \leq \frac{1}{C}\mathrm{d}(\mathbf{x}, \partial\Omega), \qquad \mathbf{x} \in \Omega, \qquad (32)$$

and so $\psi(\mathbf{x}) \to 0$ as $\mathbf{x} \to \partial\Omega$, and so ψ extends continuously to $\partial\Omega$ with value zero there. Figure 5 shows the upper and lower bounds on ψ with $C = 2$ in the case that Ω is the unit disk. The figure shows a plot of ψ and the two bounds along the x-axis. Next we show that the normal derivative of ψ is non-zero.

Theorem 5 *If* $\mathrm{d}(M_E, \partial\Omega) > 0$ *and* $\mathrm{d}(M_I, \partial\Omega) > 0$ *and* $\mathbf{y} \in \partial\Omega$, *then*

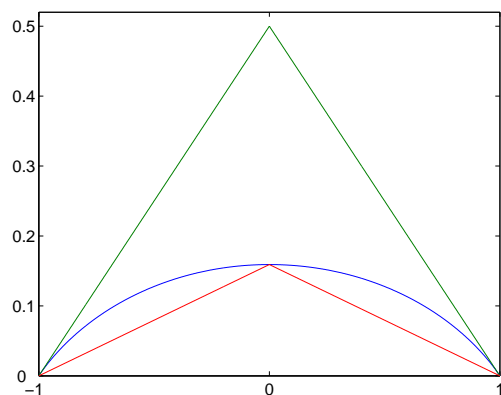$$\frac{\partial \psi}{\partial \mathbf{n}}(\mathbf{y}) = \frac{1}{2}.$$

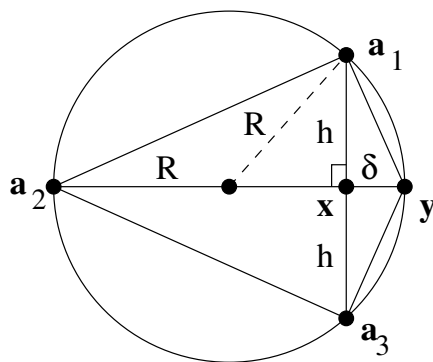Figure 5: Upper and lower bounds for the unit disk.

Figure 6: Lines in proof of Theorem 5.

15

Proof. Let $R = \mathrm{d}(M_I, \partial\Omega)$. Then the open disc B of radius R that is tangential to $\partial\Omega$ at $\mathbf{y}$ on the inside of $\partial\Omega$ is empty. For small enough $\delta > 0$, the point $\mathbf{x} = \mathbf{y} + \delta\mathbf{n}$ is in B. Let $\mathbf{a}_1, \mathbf{a}_2, \mathbf{a}_3$ be the three points on ∂B such that $\mathbf{a}_2 \neq \mathbf{y}$ lies on the line through $\mathbf{x}$ and $\mathbf{y}$, and $\mathbf{a}_1$ and $\mathbf{a}_3$ lie on the line perpendicular to it, see Figure 6. Let $\mathbf{q}$ be the four-sided polygon passing through $\mathbf{y}, \mathbf{a}_1, \mathbf{a}_2, \mathbf{a}_3$. Then

$$\phi(\mathbf{x}) \leq \int_0^{2\pi} \frac{1}{\rho_1(\mathbf{x}, \theta)} \, d\theta \leq \int_0^{2\pi} \frac{1}{\rho(\mathbf{x}, \theta; \mathbf{q})} \, d\theta.$$

Then, by Lemma 1 applied to each edge of $\mathbf{q}$, and since $\tan(\pi/4) = 1$, we have

$$\phi(\mathbf{x}) \leq 2 \left(\frac{1}{\|\mathbf{y} - \mathbf{x}\|} + \frac{1}{\|\mathbf{a}_1 - \mathbf{x}\|} \right) + 2 \left(\frac{1}{\|\mathbf{a}_1 - \mathbf{x}\|} + \frac{1}{\|\mathbf{a}_2 - \mathbf{x}\|} \right).$$

So, since $\|\mathbf{y} - \mathbf{x}\| = \delta$ and $\|\mathbf{a}_2 - \mathbf{x}\| = 2R - \delta$, and letting $h = \|\mathbf{a}_1 - \mathbf{x}\| = \|\mathbf{a}_3 - \mathbf{x}\|$, we find

$$\delta\phi(\mathbf{x}) \leq 2 \left(1 + \frac{2\delta}{h} + \frac{\delta}{2R - \delta} \right).$$

Moreover, since $h^2 = R^2 - (R - \delta)^2$, we have $h = \sqrt{(2R - \delta)\delta} \approx \sqrt{2R\delta}$ for small δ, and therefore

$$\limsup_{\delta \to 0} \delta\phi(\mathbf{x}) \leq 2. \tag{33}$$

On the other hand, for small δ, $\mathbf{y}$ is the closest point to $\mathbf{x}$ in $\partial\Omega$, and then (17) gives

$$\delta\phi(\mathbf{x}) \geq \left(\frac{2d}{\delta + d} \right) \left(\frac{d}{\delta + d + \sqrt{\delta^2 + 2\delta d}} \right),$$

where $d = \mathrm{d}(M_E, \partial\Omega)$, and thus

$$\liminf_{\delta \to 0} \delta\phi(\mathbf{x}) \geq 2. \tag{34}$$

The inequalities (33) and (34) show that $\delta\phi(\mathbf{x}) \to 2$ as $\delta \to 0$, and thus

$$\frac{\partial\psi}{\partial\mathbf{n}}(\mathbf{y}) = \lim_{\delta \to 0} \frac{\psi(\mathbf{x}) - \psi(\mathbf{y})}{\delta} = \lim_{\delta \to 0} \frac{1}{\delta\phi(\mathbf{x})} = \frac{1}{2}.$$

$\square$

We have now shown that the Hermite construction (29) works, and that the normal derivative of ψ is $1/2$. To apply (31) we still have to compute the normal derivative of g_0.

Theorem 6 *Let g be as in* (11). *If $\mathrm{d}(M_E, \partial\Omega) > 0$ and $\mathrm{d}(M_I, \partial\Omega) > 0$, and $\mathbf{y} \in \partial\Omega$ then*

$$\frac{\partial g}{\partial\mathbf{n}}(\mathbf{y}) = \frac{1}{2} \int_a^b w(\mathbf{y}, t) \big(f(\mathbf{c}(t)) - f(\mathbf{y}) \big) \, dt.$$

Proof. For small $\delta > 0$, let $\mathbf{x} = \mathbf{y} + \delta\mathbf{n}$. Then dividing both sides of equation (19) by δ, and letting $\delta \to 0$, gives the result, using Theorem 5. $\square$
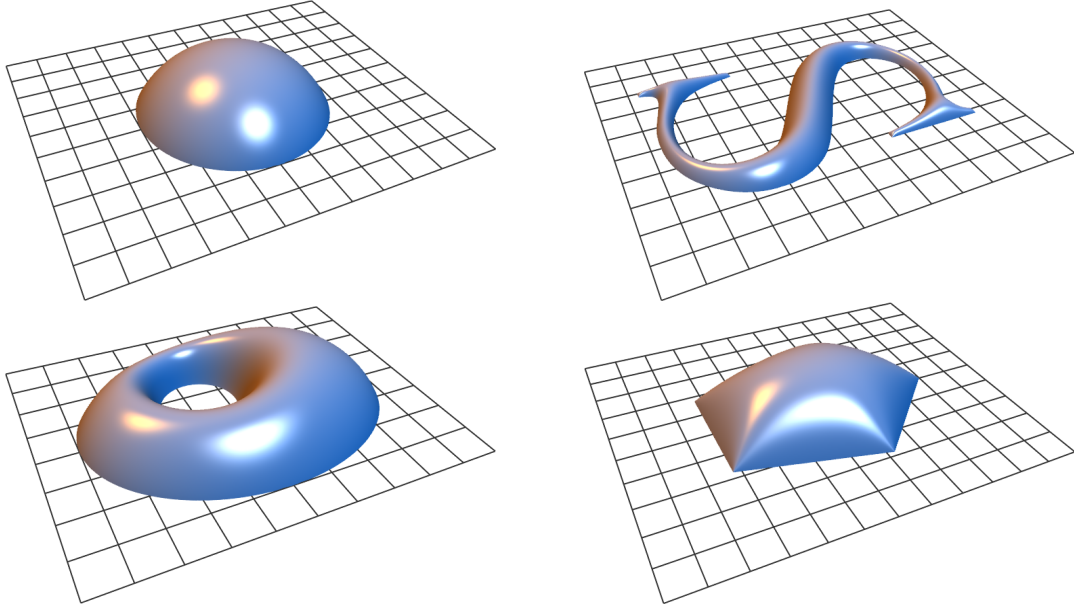
Figure 7: The weight function ψ on various domains.

We plotted the weight function ψ on four different domains, shown in Figure 7. In the first three, we used numerical quadrature on the integral formula for ϕ in (11). We use an adaptive approach, where for each $\mathbf{x}$, we split the integral into a fixed number of pieces, and apply Romberg integration to each piece, i.e., the extrapolated trapezoidal rule. If at some stage we detect that $\mathbf{x}$ is on the boundary, within a given numerical tolerance, we terminate the integration and return 0 for the value of ψ. For the fourth domain, which is a regular pentagon, we simply use the exact polygonal formula in (7). We apply similar approaches to evaluate the interpolant g in (11).

The weight function ψ is itself a Hermite interpolant with value 0 and normal derivative $1/2$ on the boundary. Figure 8 shows other Hermite interpolants.

5 A minimum principle

A useful property of harmonic functions is that they have no local maxima or minima on arbitrary domains. Lagrange mean value interpolants, however, do not share this property on arbitrary domains, but we conjecture that they do on convex domains. We are not able to show this, but we can establish a 'minimum principle' for the weight function ψ on arbitrary domains. Since ψ is positive in Ω and zero on $\partial\Omega$, it must have at least one maximum in Ω, and the S example in Figure 7 illustrates that it can have saddle points. But we show that it never has local minima.

Lemma 2 *For arbitrary Ω, with ϕ given by (14),*

$$\Delta\phi(\mathbf{x}) = 3\int_0^{2\pi} \sum_{j=1}^{n(\mathbf{x},\theta)} \frac{(-1)^{j-1}}{\rho_j^3(\mathbf{x},\theta)}\, d\theta.$$
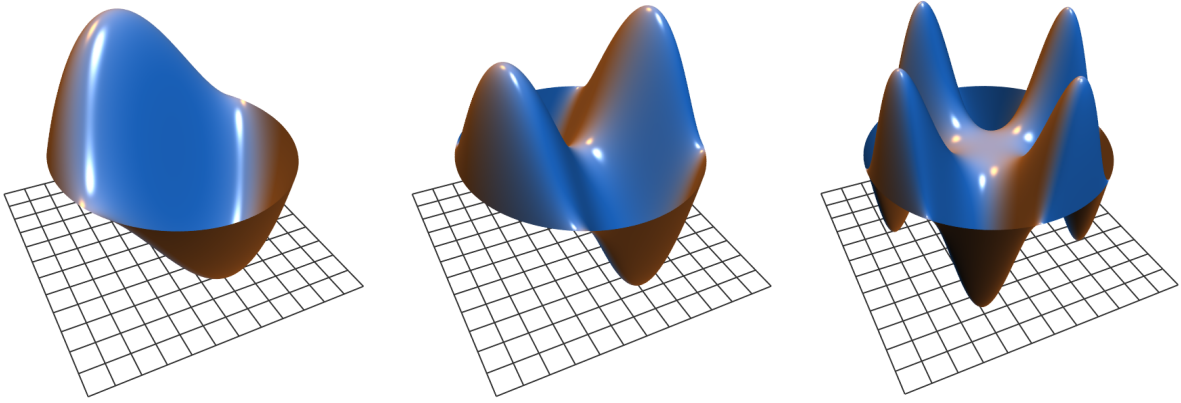
17

Figure 8: Hermite mean value interpolants.

Proof. With the notation of (22) we have $w = (\mathbf{d} \times \mathbf{c}')/r^3$ in (11) and differentiation gives

$$\nabla w = \frac{(-c_2', c_1')}{r^3} + \frac{3(\mathbf{d} \times \mathbf{c}')\mathbf{d}}{r^5} \qquad \text{and} \qquad \Delta w = 3\frac{\mathbf{d} \times \mathbf{c}'}{r^5}.$$

Integrating the latter expression with respect to t and using (10) and the notation of (14), gives the claimed formula. $\qquad\square$

Lemma 2 shows that $\Delta\phi > 0$ in Ω due to (13). From this we deduce

Theorem 7 *In an arbitrary domain Ω, the weight function ψ has no local minima.*

Proof. Suppose $\mathbf{x}_* \in \Omega$ is a local minimum of ψ. Then $\nabla\psi(\mathbf{x}_*) = \mathbf{0}$ and $\Delta\psi(\mathbf{x}_*) \geq 0$. But since $\psi = 1/\phi$, we have

$$\nabla\psi = -\frac{\nabla\phi}{\phi^2} \qquad \text{and} \qquad \Delta\psi = -\frac{\Delta\phi}{\phi^2} + 2\frac{|\nabla\phi|^2}{\phi^3}.$$

Therefore, $\nabla\phi(\mathbf{x}_*) = \mathbf{0}$ and $\Delta\psi(\mathbf{x}_*) = -\Delta\phi(\mathbf{x}_*)/\phi^2(\mathbf{x}_*) < 0$, which is a contradiction. $\qquad\square$

6 Domains with holes

So far in the paper, we have assumed that Ω is simply connected. In the case that Ω is multiply connected, all the previously derived properties and formulas continue to hold with only minor changes. In fact, the angle formula for g in (14) is unchanged in the presence of holes as long as the points $\mathbf{p}_j(\mathbf{x}, \theta)$ are understood to be the ordered intersections of $L(\mathbf{x}, \theta)$ with all components of $\partial\Omega$. Thus, all angle formulas and associated properties are also valid for multiply connected domains. However, the boundary integral formula (11) needs to be extended as follows. Suppose that Ω has m holes, $m \geq 0$, so that $\partial\Omega$ has $m + 1$ components: the outer one and the m inner ones. We represent all these pieces parametrically as $\mathbf{c}_k : [a_k, b_k] \to \mathbb{R}^2$, $k = 0, 1, \ldots, m$,
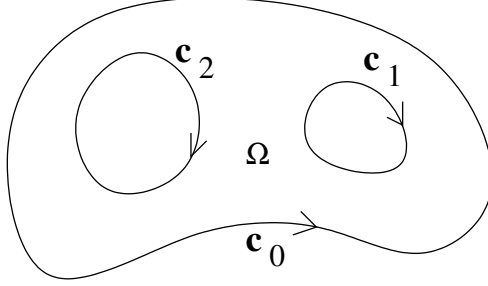
Figure 9: Multiply connected domain.

with $\mathbf{c}_k(a_k) = \mathbf{c}_k(b_k)$. The outer curve $\mathbf{c}_0$ of $\partial\Omega$ is oriented anti-clockwise and the inner pieces $\mathbf{c}_1, \ldots, \mathbf{c}_m$ are oriented clockwise, see Figure 9. Then (11) should be replaced by

$$g(\mathbf{x}) = \sum_{k=0}^{m} \int_{a_k}^{b_k} w_k(\mathbf{x}, t) f(\mathbf{c}_k(t)) \Big/ \phi(\mathbf{x}), \qquad \phi(\mathbf{x}) = \sum_{k=0}^{m} \int_{a_k}^{b_k} w_k(\mathbf{x}, t)\, dt. \qquad (35)$$

Previous formulas involving the single parametric curve $\mathbf{c}$ need to be extended accordingly, but this is straightforward and left to the reader.

7   Applications

We discuss two applications of mean value Hermite (and Lagrange) interpolation.

7.1   Smooth mappings

Smooth mappings from one planar region to another are required in reduced basis element methods for PDE's that model complex fluid flow systems [18]. The reduced basis element method is a domain decomposition method where the idea is to decompose the computational domain into smaller blocks that are topologically similar to a few reference shapes. We propose using mean value interpolation as an efficient way of generating suitable smooth mappings. Figure 10 shows on the top left a reference shape for a bifurcation point in a flow system studied in [18] that could model for example blood flow in human veins. Top right shows the reference shape mapped to the computational domain, using the method of [18]. The mapping is continuous but not C^1 along certain lines in the interior of the domain. However, the result of using Lagrange mean value interpolation is a C^∞ mapping, bottom left. Finally, it may be desirable to control the normal derivative of the mapping along the boundary. This can be achieved using Hermite mean value interpolation. Bottom right shows the Hermite mean value mapping where the normal derivative of the mapping at each boundary point equals the unit normal vector at the corresponding point of the computational domain boundary.

There appears to be no guarantee that these mappings will in general be one-to-one. However, we have tested Lagrange mean value mappings from convex domains to convex domains and have always found them to be injective. We conjecture that this holds for all convex domains.
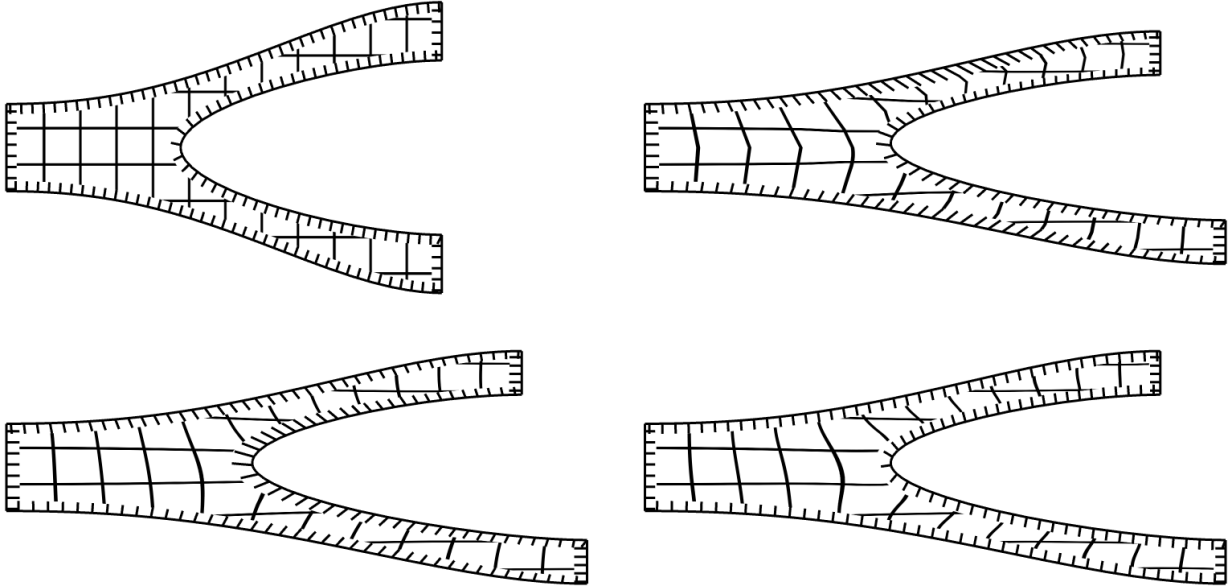
Figure 10: A bifurcation prototype is mapped to a deformed bifurcation using different transfinite interpolants.

7.2 A weight function for web-splines

Recently, Hollig, Reif, and Wipper [9, 8] proposed a method for solving elliptic PDE's over arbitrarily shaped domains based on tensor-product B-splines defined over a square grid. In order to obtain numerical stability, the B-splines are 'extended', and in order to match the zero boundary condition, they are multiplied by a common weight function: a function that is positive in Ω and zero on $\partial\Omega$. Various approaches to choosing a weight function for this kind of finite element method have been discussed in [14, 19, 9, 21]. The weight function ψ we used in Hermite interpolation satisfies these basic properties, and in view of the upper and lower bounds (32) and the constant normal derivative in Theorem 5, it behaves like half the signed distance function near the boundary. So ψ is a good candidate for the weight function in the web-spline method.

We used bicubic web-splines to solve Poisson's equation $\Delta u = f$ on various domains Ω with zero Dirichlet boundary condition and various right-hand sides f. The top two plots of Figure 11 show approximate solutions u over an elliptic domain with a circular hole, defined by the zeros of r_1 and r_2 where

$$r_1(x_1, x_2) = 1 - x_1^2/16 - x_2^2/9, \qquad r_2(x_1, x_2) = (x_1 + 3/4)^2 + (x_2 - 1/2)^2 - 1,$$

and with right hand side $f = \sin(r_1 r_2/2)$, a test case used in [9]. The top left plot shows the result of using the weight function $\psi = r_1 r_2$, while the top right plot shows the result of using the mean value weight function ψ. The error for the two methods is similar, with both having a numerical L_2-error of the order $O(h^4)$ with h the grid size, as predicted by the analysis of [9]. At the bottom of Figure 11 are plots of the approximate numerical solution to $\Delta u = -1$ on other domains using the mean value weight function. On the left is the solution over a regular
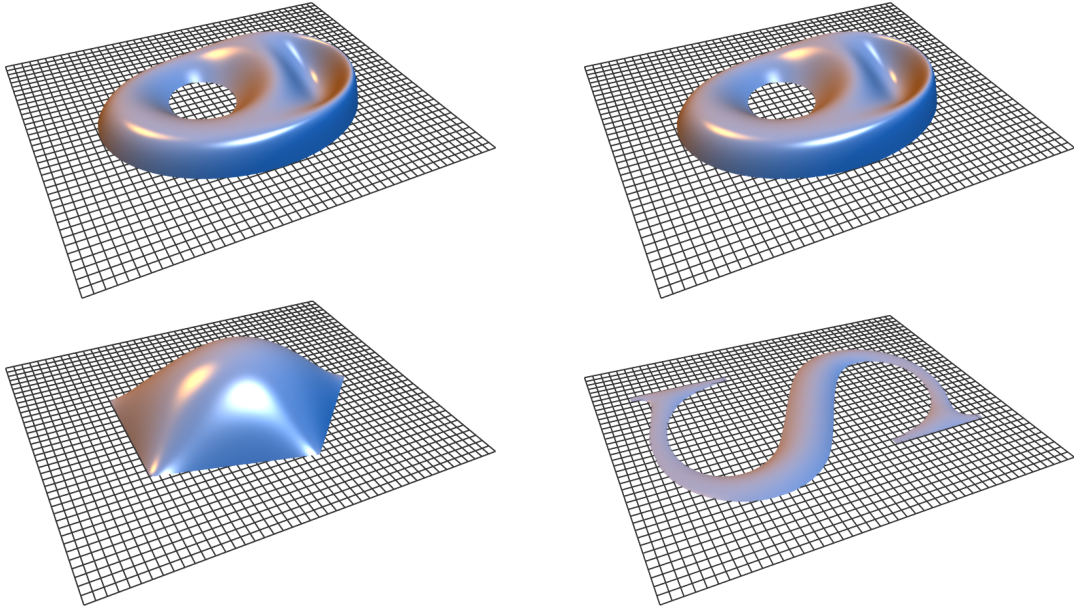
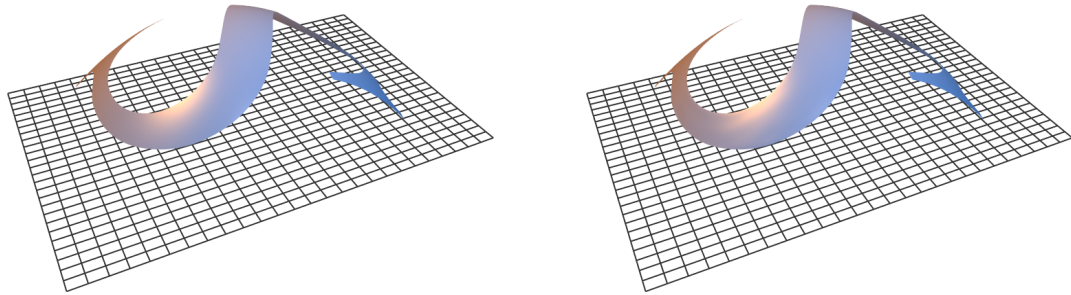Figure 11: Numerical solution using bicubic web-splines.

Figure 12: Solving inhomogeneous problems.

pentagon, and on the right is the solution over the domain defined by the 'S' in the Times font, with piecewise-cubic boundary. The numerical L_2 error in these two cases was $O(h^2)$, which is expected when the domain boundary has corners.

One can extend the web-spline method to deal with inhomogeneous problems using Lagrange mean value interpolation. If we want to solve $\Delta u = f$ in Ω with $u = u_0$ on $\partial\Omega$, we can let g be the mean value interpolant (11) to u_0, and express the solution as $u = g + v$ where v solves the homogeneous problem $\Delta v = \hat{f}$ in Ω with $v = 0$ on $\partial\Omega$, and $\hat{f} = f - \Delta g$. This approach requires computing the Laplacian of the mean value interpolant g in (4) and this can be done using the formulas of Section 3. We used bicubic web-splines to solve the inhomogeneous problem with $f = -1/2$ and $u_0(\mathbf{y}) = 1 - (y_1^2 + y_2^2)/8$. In Figure 12, the left plot shows the true solution $u(\mathbf{x}) = 1 - (x_1^2 + x_2^2)/8$ and the right plot shows the numerical solution.

and comments in this work.

References

[1] A. Belyaev, On transfinite barycentric coordinates, in *Eurographics symposium on geometry processing*, K. Polthier and A. Sheffer (eds.), 2006, pp 89–99.

[2] H. Blum, A transformation for extracting new descriptors of shape, in *Models for the perception of speech and visual form*, W. Wathen-Dunn (ed.), MIT (1967), 362–380.

[3] M. S. Floater, Mean value coordinates, Comp. Aided Geom. Design **20** (2003), 19–27.

[4] M. S. Floater, K. Hormann, and G. Kos, A general construction of barycentric coordinates over convex polygons, Adv. in Comp. Math. **24** (2006), 311–331.

[5] M. S. Floater and K. Hormann, Barycentric rational interpolation with no poles and high rates of approximation, to appear in Numerische Mathematik.

[6] M. S. Floater, G. Kos, and M. Reimers, Mean value coordinates in 3D, Comp. Aided Geom. Design **22** (2005), 623-631.

[7] W. J. Gordon and J. A. Wixom, Pseudo-harmonic interpolation on convex domains, SIAM J. Numer. Anal. **11** (1974), 909–933.

[8] K. Hollig, *Finite element methods with B-splines*, SIAM, 2003.

[9] K. Hollig, U. Reif, and J. Wipper, Weighted extended B-spline approximation of Dirichlet problems, SIAM J. Numer. Anal. **39** (2001), 442–462.

[10] K. Hormann and M. S. Floater, Mean value coordinates for arbitrary planar polygons, ACM Trans. on Graphics 25 (2006), 1424–1441.

[11] T. Ju, P. Liepa, and J. Warren, A general geometric construction of coordinates in a convex simplicial polytope, CAGD **24** (2007), 161–178.

[12] T. Ju, S. Schaefer, and J. Warren, Mean value coordinates for closed triangular meshes, ACM TOG **24** (2005), 561–566.

[13] T. Ju, S. Schaefer, J. Warren, and M. Desbrun, A geometric construction of coordinates for convex polyhedra using polar duals, in *Geometry Processing 2005*, M. Desbrun and H. Pottman (eds.), Eurographics Association 2005, 181–186.

[14] L. V. Kantorovich and V. I. Krylov, *Approximate methods of higher analysis*, Interscience, 1964.

[15] T. Langer, A. Belyaev, and H.-P. Seidel, Spherical barycentric coordinates, in *Eurographics symposium on geometry processing*, K. Polthier and A. Sheffer (eds.), 2006, pp 81–88.

[16] S. L. Lee, Mean value representations and curvatures of compact convex hypersurfaces, preprint, 2007.

[17] Y. Lipman, J. Kopf, D. Cohen-Or, and D. Levin, GPU-assisted positive mean value coordinates for mesh deformation, to appear in the Symposium on Geometry Processing, 2007.

[18] A. E. Løvgren, Y. Maday, and E. M. Rønquist, A reduced basis element method for complex flow systems, in *European Conference on Computational Fluid Dynamics*, P. Wesseling, E. Onate, and J. Periaux (eds.), TU Delft, The Netherlands, 2006.

[19] V. L. Rvachev, T. I. Sheiko, V. Shapiro, and I. Tsukanov, Transfinite interpolation over implicitly defined sets, Comp. Aided Geom. Design **18** (2001), 195–220.

[20] M. Sabin, Transfinite surface interpolation, in *Mathematics of Surfaces VI*, G. Mullineux (ed.), Clarendon Press, 1996, pp 517–534.

[21] V. Shapiro, Semi-analytic geometry with R-functions, Acta Numerica (2007), 1–65.

[22] J. Warren, S. Schaefer, A. Hirani and M. Desbrun, Barycentric coordinates for convex sets, to appear in Adv. in Comp. Math.